

Moving up and down the Titanium Oxidation State in Ziegler–Natta Catalysis

Naeimeh Bahri-Laleh,^{*,†} Andrea Correa,[‡] Shahram Mehdipour-Ataei,[†] Hassan Arabi,[†] Mehdi Nekoomanesh Haghghi,[†] Gholamhosein Zohuri,[§] and Luigi Cavallo^{*,‡}

[†]*Iran Polymer and Petrochemical Institute (IPPI), Polymerization Engineering Department, P.O. Box 14965/115, Tehran, Iran,* [‡]*Department of Chemistry, University of Salerno, Via Ponte don Melillo, Fisciano I-84084, Italy,* and [§]*Chemistry Group, Department of Science, Ferdowsi University, Mashhad-91775, I. R. Iran*

Received October 16, 2010; Revised Manuscript Received December 16, 2010

ABSTRACT: DFT molecular modeling studies were undertaken to shed light on possible activation and deactivation mechanisms of Ziegler–Natta catalytic systems, as well as on the possible mechanisms for their reactivation by organohalides. We focused our efforts on Ti species attached to the (110) lateral cut of MgCl₂. First, the possible activation of adsorbed TiCl₄ leading to an adsorbed Ti^{III} species bearing a Ti–alkyl bond and a coordination vacancy, which is a species able to undergo chain-growth, was considered. According to our calculations formation of the first active species can be easily rationalized by cleavage of a Ti–Cl bond of coordinated TiCl₄ by AlEt₃, followed by transalkylation promoted by another AlEt₃ molecule. Second, we investigated the possible reduction of polymerization active Ti^{III} species leading to polymerization inactive Ti^{II} species, and we found that a Ti–H bond, possibly formed after chain termination, is weaker than the Ti–Et (polymeryl) bond. Third, we investigated the mechanism of reactivation of Ti^{II} species by organohalides, and it was concluded that reoxidation by Cl rich organohalides is thermodynamically more favored.

Introduction

The discovery of Ziegler–Natta (ZN) polymerization in 1953 is probably the most important achievement in the field of synthetic polymer chemistry during the past half-century.^{1,2} Modern ZN catalysts for the industrial production of polyolefins are based on TiCl₄ supported on activated MgCl₂.³ Yet, despite more than 50 years have passed, the mechanism of polymerization from Ti activation to its deactivation included, is still not fully understood. This situation despite of several experimental^{4–9} and theoretical^{10–15} studies has provided remarkable insight. The picture emerging from the above characterization studies supports the formation of preferential cuts on MgCl₂ crystallites corresponding to the more stable (104) and less stable (110) planes.^{13,16} On these coordinatively unsaturated Mg²⁺ ions the chemisorption of TiCl₄ molecules is likely to occur and a variety of active site structures have been proposed.^{17,18} However, calculations indicate that TiCl₄ coordination to the (104) plane is rather weak or even unstable, whereas TiCl₄ coordination to the (110) plane is energetically quite favored.^{19–22} This raises the hypothesis that the polymerization active TiCl₄ actually coordinates to the less stable (110) plane. Further, models have been proposed that explain in a simple way the stereoselective induction promoted by Lewis bases when coordinated in the near proximity of a TiCl₄ molecule adsorbed on the less stable (110) plane.²³ These results suggest that the active Ti atoms might be coordinated on the (110) plane or could have a local environment similar to that assumed after coordination on the (110) plane. For this reasons, an octahedral Ti atom adsorbed on the (110) plane is becoming sort of a good model of the real active species. As mentioned before, this model has been used to rationalize the role of the Lewis bases in conferring the experimentally observed stereoselectivity in both primary^{24–26} and secondary²⁷ propene insertion. Further, in the

framework of the three sites model, an octahedral Ti atom adsorbed on the (110) plane can easily rationalize the presence of the majority of stereomistakes into block of lower stereoregularity.^{27,28}

However, this reasonably good understanding of the behavior of this possible active species during chain growth is counterbalanced by the scarce knowledge we have of the activation steps, and of the way the initial Ti^{IV} atom of the adsorbed TiCl₄ molecule is reduced to Ti^{III}, and the way the first Ti–C bond is formed by reaction of the adsorbed Ti species with the Al cocatalyst. Indeed, it is well-known that in ZN polymerization of both ethene and propene the Ti atoms exist in several oxidation states, +2, +3, and +4, and the well-accepted idea is that Ti^{III}, formed from reduction of Ti^{IV}, is the active oxidation state, whereas further reduction to Ti^{II} greatly reduces polymerization activity, or actually completely deactivates the metal center.^{29,30} The most used approach to reactivate the Ti^{II} centers back to Ti^{IV} is to add organohalides, such as CCl₄, CHCl₃, ClCH₂CH₂Cl, chlorocyclohexane, or even Cl₂, as oxidizing agents.^{31,32} The restored Ti^{IV} centers can be activated again, which increases the overall activity.³³ Following this scheme, Cl containing compounds or organohalides has been commonly used as activity promoters for vanadium based,^{34–36} and titanium based ZN catalysts.^{37,38}

Despite the relevance of the activation step, and of the possible ways in which the Ti center can be oxidized and/or reduced, little efforts have been performed from a theoretical point of view to shed light on these points. The most noticeable exception is a recent and valuable study that offered a reasonable overview of the activation steps.³⁹ However, this study often relies on bimetallic models that possibly can be present during activation, but we still believe that activation should preferentially occur on a monometallic Ti species. Further, deactivation to Ti^{II}, as well as the possible reactivation via oxidation by halocompounds, was not investigated.

In this contribution, we try to fill this gap, and DFT studies were undertaken in the attempt to shed light on possible pathways for

*Corresponding authors. E-mail: (L.C.) lcavallo@unisa.it.

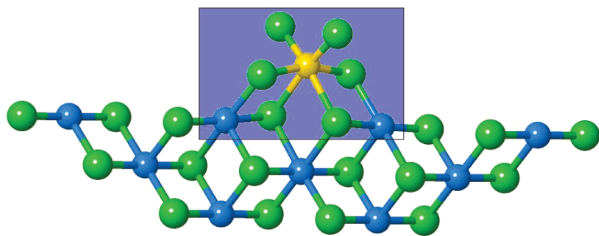


Figure 1. Structure of TiCl_4 adsorbed on the $(\text{MgCl}_2)_9$ cluster. The only atoms relaxed in the geometry optimizations are those in the blue box.

the change of the Ti oxidation state from Ti^{IV} to Ti^{III} initially, with inclusion of possible pathways for the formation of the first Ti–C bond, which actually corresponds to the Ti activation. Then, we explored possible pathways that would reduce Ti^{III} to Ti^{II} , which corresponds to Ti deactivation, and finally, we explored the possible reactivity through which organohalides could reoxidize Ti^{II} to Ti^{IV} , reintroducing them into the active cycle.

In this study we focused on a TiCl_4 molecule octahedrally coordinated on the (110) MgCl_2 surface since, as previously mentioned, there is growing evidence that the real active Ti species could have a similar environment. Further, most of the reactions considered, for example the breaking of a Ti–Cl bond assisted by the Al cocatalyst, require a change of the electronic state of the Ti species from singlet to doublet. Modeling the transition state for reactions with a change in the electronic state is computationally a real challenge that would prevent to investigate the large number of reactions we considered. For this reason, in these cases we only focused on the thermodynamics of the reaction, to exclude some reactivity and highlight those reactions that can actually occur. Otherwise, when we focused on a reaction with no change in the electronic state, we followed the classical approach in which all the steps (intermediates and transition states between reactants and products) were investigated.

Models and Computational Details

Active Site Models. A semiflexible $(\text{MgCl}_2)_9$ cluster was used in all the simulations to support the monometallic Ti species; see Figure 1. The MgCl_2 bulk was assumed to be in the α crystalline phase, and the surface was modeled as a (110) monolayer. During the geometry optimizations all the atoms involved in Ti coordination were relaxed, while the remaining part of the MgCl_2 cluster was frozen in the position of the ideal crystal. For example, in case of TiCl_4 coordination the relaxed atoms are those in the blue box in Figure 1. All the systems were modeled similarly, with the exception of those to obtain the energy profile for the transalkylation reaction, where a completely relaxed $(\text{MgCl}_2)_3$ cluster was used.

In case of Ti^{IV} species the singlet electronic state is favored, and thus closed shell calculations were performed. Differently, for Ti^{III} and Ti^{II} unrestricted calculations were performed, since Ti^{III} has one unpaired electron, while for Ti^{II} we found that a triplet electronic state with two unpaired electrons is favored relative to the singlet electronic state. Unrestricted calculations were performed for all the radical species involving main group atoms.

DFT Calculations. The DFT calculations were carried out using the Turbomole 6.1⁴⁰ and the Gaussian03⁴¹ packages, and the B3LYP hybrid GGA functional of Becke–Lee, Parr, and Yang was adopted.^{42,43} The Gaussian package was used only in the direct transalkylation reaction of Figure 2, due to an easier handling of the transition state searches. In the Turbomole calculations the electronic configuration of the atoms was described by a triple- ζ basis set augmented with

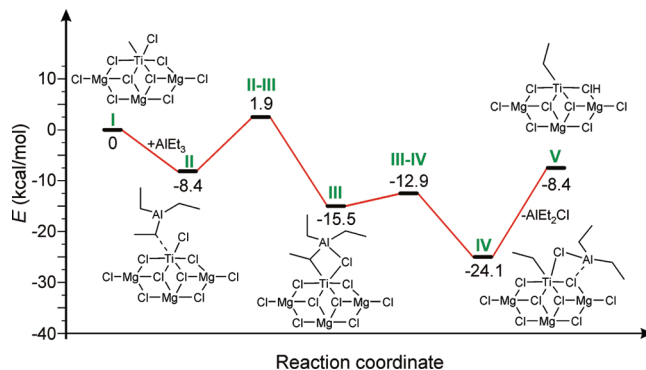


Figure 2. Energy profile, in $\text{kcal}\cdot\text{mol}^{-1}$, of the direct transalkylation reaction.

Table 1. Thermodynamics of the Homolytic Dissociation, ΔE_{diss} in $\text{kcal}\cdot\text{mol}^{-1}$, of a Cl Atom from an Adsorbed TiCl_4

	reaction	ΔE_{diss}
1	$\text{TiCl}_4 \rightarrow \text{TiCl}_3^{\bullet} + \text{Cl}^{\bullet}$	83.1
2	$[\text{Mg}]/\text{TiCl}_4 \rightarrow [\text{Mg}]/\text{TiCl}_3^{\bullet} + \text{Cl}^{\bullet}$	62.3
3	$[\text{Mg}]/\text{TiCl}_4 + \text{AlCl}_3 \rightarrow [\text{Mg}]/\text{TiCl}_3^{\bullet} + \text{AlCl}_4^{\bullet}$	42.5
4	$[\text{Mg}]/\text{TiCl}_4 + \text{Al}_2\text{Cl}_6 \rightarrow [\text{Mg}]/\text{TiCl}_3^{\bullet} + \text{Al}_2\text{Cl}_7^{\bullet}$	54.0
5	$[\text{Mg}]/\text{TiCl}_4 + \text{AlEt}_3 \rightarrow [\text{Mg}]/\text{TiCl}_3^{\bullet} + \text{AlEt}_3\text{Cl}^{\bullet}$	8.8
6	$[\text{Mg}]/\text{TiCl}_4 + \text{Al}_2\text{Et}_6 \rightarrow [\text{Mg}]/\text{TiCl}_3^{\bullet} + \text{AlEt}_3 + \text{AlEt}_3\text{Cl}^{\bullet}$	25.8 ^a
7	$[\text{Mg}]/\text{TiCl}_4 + \text{CH}_2\text{CH}_2 \rightarrow [\text{Mg}]/\text{TiCl}_3^{\bullet} + \text{CH}_2\text{CH}_2\text{Cl}^{\bullet}$	44.8

^a Assuming a value of $17 \text{ kcal}\cdot\text{mol}^{-1}$ for the enthalpy of dissociation of Al_2Et_6 .⁴⁶

two polarization functions (Turbomole basis set TZVPP).⁴⁴ In the Gaussian03 calculations the triple- ζ basis set augmented with one polarization functions of Ahlrichs and co-workers was used (TZVP keyword in Gaussian).⁴⁵

Results and Discussion

Formation of the First Vacancy on Ti. Considering the chemical species in the polymerization medium, three principal different paths can be envisaged for the reduction of adsorbed TiCl_4 . All of them basically consist of the homolytic breaking of a dangling Ti–Cl bond: (i) Spontaneous dissociation; (ii) dissociation induced by a reducing agent such as AlCl_3 , Al_2Cl_6 , and AlEt_3 ; (iii) dissociation promoted by C_2H_4 . The thermodynamics of these reactions is reported in Table 1.

To understand better the role of the support in assisting dissociation of the Ti–Cl bond, we first calculated the ΔE_{diss} of the Ti–Cl bond in free TiCl_4 , $83.1 \text{ kcal}\cdot\text{mol}^{-1}$, entry 1 in Table 1. The spontaneous dissociation of Ti–Cl bond of a TiCl_4 molecule adsorbed on a MgCl_2 layer, entry 2 in Table 1, still is highly endothermic, $62.3 \text{ kcal}\cdot\text{mol}^{-1}$, indicating that the MgCl_2 support scarcely assists the homolytic breaking of a Ti–Cl bond, excluding thus the spontaneous pathway. Moving to dissociation assisted by Al compounds as acceptors of the extracted Cl atom, the monomeric AlCl_3 , entry 3 in Table 1, reduces ΔE_{diss} to $42.5 \text{ kcal}\cdot\text{mol}^{-1}$, while the dimeric form, entry 4 in Table 1, with a ΔE_{diss} of $54.0 \text{ kcal}\cdot\text{mol}^{-1}$, is less effective. This can be related to the more acidic behavior of monomeric AlCl_3 . Nevertheless these numbers indicate that the reduction process promoted by either monomeric or dimeric Al–chloride compounds remains thermodynamically very unfavored. This finding is consistent with Skalli's results, who suggested that AlCl_3 does not assist reduction of TiCl_4 .³³

Since AlEt_3 is the most used reducing agent in ZN catalysis, we explored to which extent Al–alkyl compounds are better than Al–chlorides compounds to promote Ti–Cl dissociation. In the presence of AlEt_3 , entry 5 in Table 1, ΔE_{diss} amounts to

8.8 kcal·mol⁻¹ only. A value that is far smaller than that calculated for AlCl₃, and a value that can be easily reached by moderate heating of the reaction media.

Since AlEt₃ is dimeric (the dimerization enthalpy in hexadecane is 17 kcal mol⁻¹),^{46,47} Ti activation promoted by Al-alkyl compounds first requires dissociation of Al₂Et₆, and this energetic cost should be added to the ΔE_{diss} of Table 1, which results in an approximated ΔE_{diss} of 25.8 kcal mol⁻¹, entry 6 in Table 1. Nevertheless, it is worth noting that the free energy of dissociation of Al₂Et₆ should roughly cost 7 kcal mol⁻¹ (the enthalpy of dissociation, 17 kcal mol⁻¹, minus roughly 10 kcal mol⁻¹ as the entropy gain for dissociation of a bimolecular species), which should result in a fraction of monomeric AlEt₃ present in the reaction media.⁵⁰

The ability of AlEt₃ to assist dissociation of a Ti-Cl bond is in the oxidative power of the liberated Cl atom, that attacks the Al center by nearly expelling one rather stable Et radical. This conclusion is supported by the strong exothermicity of the AlEt₃ + Cl[•] → AlEt₃Cl[•] reaction, 46.9 kcal mol⁻¹, and by the strong asymmetric elongation of the Al-Et bonds in AlEt₃Cl[•]. In fact, while two of the Al-Et bonds in AlEt₃Cl[•] are substantially unchanged from the value of 1.99 Å in AlEt₃, the third Al-Et bond is 2.42 Å long.

These results indicate that AlEt₃, besides being needed to initiate the polymerization process by formation of the first Ti-C bond, facilitates the reduction process.³³ Further, the ΔE_{diss} we calculated for the dissociation of a Ti-Cl bond assisted by AlEt₃ is smaller than the energy required to dissociate the O-O bond of benzyl peroxide, 22.7 kcal·mol⁻¹, a classical radical initiator with a half-life time of 7.2 min in toluene at 100 °C.

Finally, we also investigated if the monomer, which is the predominant species in the polymerization medium, could promote dissociation of the Ti-Cl bond. Interestingly, the ΔE_{diss} of a Ti-Cl bond assisted by ethylene, 44.8 kcal·mol⁻¹, entry 6 in Table 1, compares well with the ΔE_{diss} of AlCl₃, and seems to be more effective than Al₂Cl₆. Nevertheless, of all the dissociation processes we considered, the only one that seems viable is that assisted by AlEt₃, either as a monomer or as a dimer.

Formation of the First Ti-C Bond. After having explored the possible pathways for the formation of the first vacancy on Ti, with reduction of Ti^{IV} to Ti^{III}, we moved to the possible pathways leading to formation of a Ti-C bond. We considered two mechanisms: (i) transalkylation by AlEt₃, which would form in a single step the Ti^{III} active species with a Ti-C bond and a vacancy on the Ti atom ready for monomer coordination; (ii) a two steps mechanism with reoxidation of the Ti^{III} center by AlEt₃Cl[•] formed during activation by AlEt₃ first, followed by homolytic dissociation of the remaining Ti-Cl dangling bond. These paths are shown in Scheme 1.

Direct transalkylation, entry 1 in Table 2, is favored by 4.4 kcal·mol⁻¹, which indicates the thermodynamic feasibility of this reaction. Considering that direct transalkylation does not require a change in the spin state, we decided to investigate the exact mechanism. For these calculations we abandoned the semiflexible MgCl₂-cluster approximation and, as described in the Models and Computational Details, all the atoms have been relaxed. The energy profile is reported in Figure 2.

The first step is coordination of AlEt₃ to the Ti center through an ethyl group. The corresponding coordination intermediate **II** is 8.4 kcal·mol⁻¹ below the separated species, indicative of an already reasonable interaction between the Ti and AlEt₃. The reaction proceeds through transition states **II-III**, at 10.3 kcal·mol⁻¹ above **II**, in which the Al

Scheme 1

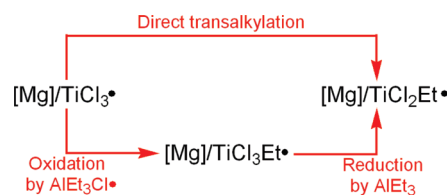


Table 2. Thermodynamics, in kcal·mol⁻¹, Associated with the Formation of the First Ti-C Bond

	reaction	ΔE
1	[Mg]/TiCl ₃ • + AlEt ₃ → [Mg]/TiCl ₂ Et• + AlEt ₂ Cl	-4.4
2	[Mg]/TiCl ₃ • + AlEt ₃ Cl [•] → [Mg]/TiCl ₃ Et + AlEt ₂ Cl	-19.2
3	[Mg]/TiCl ₃ Et → [Mg]/TiCl ₂ Et• + Cl [•]	68.3
4	[Mg]/TiCl ₃ Et → [Mg]/TiCl ₃ • + Et•	25.8
5	[Mg]/TiCl ₃ Et + AlEt ₃ → [Mg]/TiCl ₂ Et• + AlEt ₃ Cl [•]	14.9
6	[Mg]/TiCl ₃ Et + AlEt ₃ → [Mg]/TiCl ₃ • + AlEt ₄ •	21.4

center attacks the dangling Cl atom, leading to intermediate **III**, which lies 15.5 kcal·mol⁻¹ below the starting species **I**. Intermediate **III** is a bridged structure in which one of the Et groups and the Cl atom connect the Al and the Ti centers. The breaking of intermediate **III** occurs through transition state **III-IV**, at 2.6 kcal·mol⁻¹ above **III**, and leads to intermediate **IV**, 24.1 kcal·mol⁻¹ below the starting species **I**, due to a strong interaction between the Al center and one Cl atoms bridging the Ti center to the support. Dissociation of AlEt₂Cl from **IV** leads to **V**, which is the starting point for chain growth. In case of the relaxed MgCl₂ cluster the transalkylation step from **I** to **V** is favored by 8.4 kcal·mol⁻¹, while in case of the rigid MgCl₂ cluster model it was favored by 4.4 kcal·mol⁻¹, entry 1 in Table 2, which indicates that the exact model used has not a dramatic effect on the calculated energies.

The second possible mechanism for the formation of the first Ti-C bond is related to the reaction of [Mg]/TiCl₃• with AlEt₃Cl[•]; see Scheme 1. Since this two steps mechanism involves a change in the spin state, we only considered the thermodynamic feasibility of the two steps. As expected, the former step, which corresponds to the association of two radical species, is strongly favored (by 19.2 kcal·mol⁻¹, entry 2 in Table 2). This step leads to the formation of [Mg]/TiCl₃Et, which can undergo to either Ti-Cl dissociation, leading to the [Mg]/TiCl₂Et• active species, or Ti-Et dissociation, leading back to [Mg]/TiCl₃•. The Ti-Cl bond, with a ΔE_{diss} of 68.3 kcal·mol⁻¹, entry 3 in Table 2, is only 6.0 kcal·mol⁻¹ stronger than a Ti-Cl bond in [Mg]/TiCl₄, but it is far stronger than the Ti-Et bond, for which a ΔE_{diss} of only 25.8 kcal·mol⁻¹, entry 4 in Table 2, was calculated. These numbers indicate that the Ti-Et bond is by far less stable than the Ti-Cl bond, and if any spontaneous dissociation occurs this would involve the Ti-Et bond. In line with the reduction of [Mg]/TiCl₄, we explored the effect of AlEt₃ in assisting dissociation of both Ti-Cl and Ti-Et from [Mg]/TiCl₃Et. Also in this case AlEt₃ is very effective in stabilizing the formed Cl[•] atom, reducing the ΔE_{diss} of the Ti-Cl bond to 14.9 kcal·mol⁻¹, entry 5 in Table 2. Differently, the Et• radical is slightly stabilized by AlEt₃, since the ΔE_{diss} decreases to 21.4 kcal·mol⁻¹ only. Of relevance, however, is the fact that in the presence of AlEt₃ dissociation of the Ti-Cl bond is thermodynamically favored by 6.5 kcal·mol⁻¹ over dissociation of the Ti-Et bond.

Concluding this section, calculations suggest that the most likely mechanism leading to formation of the first [Mg]/TiCl₂Et• active species is direct transalkylation, which is in line with the accepted ideas in the field.

Table 3. Thermodynamics of Deactivation, ΔE_{diss} in kcal·mol⁻¹, Associated with Reduction from Ti^{III} to Ti^{II}

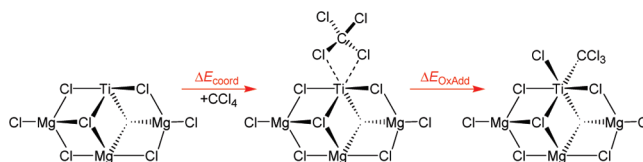
	reaction	ΔE_{diss}
1	[Mg]/TiCl ₂ Et* → [Mg]/TiCl ₂ + Et*	37.0
2	[Mg]/TiCl ₂ Et* → [Mg]/TiClEt + Cl*	109.9
3	[Mg]/TiCl ₂ H* → [Mg]/TiCl ₂ + H*	45.2
4	[Mg]/TiCl ₂ Et* → [Mg]/TiCl + EtCl	81.8
5	[Mg]/TiCl ₂ Et* + AlEt ₃ → [Mg]/TiCl ₂ + AlEt ₄ *	32.6
6	[Mg]/TiCl ₂ Et* + AlEt ₃ → [Mg]/TiClEt + AlEt ₃ Cl*	56.4
7	[Mg]/TiCl ₂ H* + AlEt ₃ → [Mg]/TiCl ₂ + AlEt ₃ H*	23.0
8	[Mg]/TiCl ₂ Et* + C ₂ H ₄ → [Mg]/TiClEt + CH ₂ ClCH ₂ *	92.4
9	[Mg]/TiCl ₂ Et* + C ₂ H ₄ → [Mg]/TiCl ₂ + C ₄ H ₉ *	16.9
10	[Mg]/TiCl ₂ H* + C ₂ H ₄ → [Mg]/TiCl ₂ + CH ₃ CH ₂ *	2.9

Deactivation of the Catalyst Active Site. As mentioned before, Ti^{III} centers are supposed to be more active than Ti^{II} centers, and catalysts deactivation is often associated with a reduction of Ti^{III} to Ti^{II}, and at least six different mechanisms were proposed:⁵¹ (i) spontaneous deactivation; (ii) deactivation by Al compounds; (iii) deactivation by the monomer; (iv) deactivation by molecular hydrogen; (v) deactivation by impurities or poison; (vi) deactivation by the electron donors. We investigated the thermodynamics of the first three deactivation mechanisms described above, while we did not consider deactivation by impurities or poison and deactivation by electron donors. Considering the rather unknown nature of the specie involved, and of actual Ti bonds that are broken, we considered the breaking of the Ti–Et bond as a model of the polymerization active species, the breaking of the Ti–H bond, which can be present after a classical β -H termination reaction or after chain termination by molecular hydrogen, and finally the breaking of a Ti–Cl bond that bridges the Ti species to the MgCl₂ surface. The energetic we obtained is reported in Table 3.

Entries 1–3 of Table 3 are an estimate of the relative strength of the bonds involved, and indicate that the Ti–Et bond, with a ΔE_{diss} of 37.0 kcal·mol⁻¹, is the weakest bond. The Ti–H bond, with a ΔE_{diss} of 45.2 is only 8.2 kcal·mol⁻¹ stronger, while extraction of a Cl atom bridging the Ti atom with the MgCl₂ surface, with a ΔE_{diss} of 109.9 kcal·mol⁻¹, is remarkably more expensive. Finally, we also considered that an Et–Cl species could be reductively eliminated, but also this possibility, entry 4 in Table 3, with a ΔE_{diss} of 81.8 kcal·mol⁻¹, is of high energy. Considering these values, it can be concluded that spontaneous dissociation of any species, with reduction to Ti^{II}, can be excluded.

The role of AlEt₃ in assisting reduction to Ti^{II} is summarized in entries 5–7 of Table 3. In line with the results of the previous section, dissociation of a Ti–Et bond, with a ΔE_{diss} of 32.6 kcal·mol⁻¹, is scarcely assisted from AlEt₃, due to the instability of the formed AlEt₄* species. Conversely, AlEt₃ is quite able to stabilize the Cl* and H* atoms, and thus dissociation of the Ti–H bond and of the bridging Ti–Cl bond, with ΔE_{diss} of 23.0 and 56.4 kcal·mol⁻¹, respectively, are quite reduced relative to the unassisted values, entries 2 and 3 in Table 3. Indeed, in presence of AlEt₃ the weakest bond is Ti–H, 9.6 kcal·mol⁻¹ weaker than the Ti–Et bond, and starts to be weak enough to represent a possible deactivation pathway in the industrially used reaction conditions.

Finally, we also investigated the possible role of the monomer, ethene in this case, to act as reducing agent, entries 8–10 in Table 3. While ethene also is unable to dissociate a Cl atom from the surface, entry 8 in Table 3, the low ΔE_{diss} of 16.9 and 2.9 kcal·mol⁻¹ for Ti–Et and Ti–H, respectively, indicates that olefins have the potential to deactivate the Ti^{III} active species by promoting either Ti–Et or Ti–H dissociation. Of course, this is possible because of the high energy gain associated with formation of the C–C and C–H bonds. However, we believe that the main reaction involving ethene will

Scheme 2

be its coordination to the Ti center, which results in an energy gain of 13.2 and 2.5 kcal mol⁻¹ in case of a Ti–H or a Ti–Et bond, respectively, followed by ethylene insertion into these bonds, rather than Ti–H or Ti–Et dissociation.

Concluding this section, calculations suggest that the most likely deactivation mechanism involves dissociation of a Ti–H bond. This conclusion is in qualitative agreement with the reduction in ethene polymerization activity observed when molecular hydrogen is added, since a higher concentration of Ti–H bonds should be formed at higher contents of molecular hydrogen. In case of propene polymerization, instead, molecular hydrogen is known to increase activity, which should be at odd with the above conclusion. However, in the case of propene polymerization, it is quite accepted that molecular hydrogen is able to reactivate a dormant site after a regiomistake.

Oxidation by Organohalides. One of the typical procedures to reactivate a Ti^{II} species consists in the addition of organohalides that are supposed to reactivate the Ti^{II} center by oxidizing it to Ti^{IV}. For this reason, in this section the oxidation of a Ti^{II} center by different organohalides was studied. The pathway we considered is shown in Scheme 2 for CCl₄.

Preliminary calculations indicated that the favored electronic state in the uncoordinated [Mg]/TiCl₂ species, as well as after organohalide coordination, is a triplet with both unpaired electrons substantially localized on the Ti^{II} center, with the singlet at least 20 kcal·mol⁻¹ higher in energy. Differently, after oxidative addition of the organohalide the favored electronic state of the resulting [Mg]/TiCl₃CH_nCl_{3-n} (n = 0–3) species is singlet, with the triplet at least 15 kcal·mol⁻¹ higher in energy. This implies that during the oxidative addition there will be a change in the electronic state of the system from triplet to singlet. For this reason, and in line with the previous sections, we limit the discussion to the thermodynamics balance of the reaction with a particular focus on a comparison between different organohalides. The calculated energies are reported in Table 4, entries 1–4. Each reaction is split between organohalide coordination to the [Mg]/TiCl₂ species and oxidative addition of the coordinate organohalide to the Ti center.

The reaction starts with the remarkable exothermic coordination (ΔE_{Coord} around 10–15 kcal·mol⁻¹) of the organohalides to the Ti^{II} center. There is a regular decreasing trend of the coordination energy with the amount of Cl atoms in the organohalide, and coordination of CCl₄ is less favored. Coordination of the organohalides having more than one Cl occurs with two Cl atoms inducing a roughly octahedral coordination around the Ti^{II} center, see Scheme 2. Natural population analysis (NPA)⁵² of the free organohalides indicates that the NPA charge on the Cl atoms is –0.08e, –0.03e, 0.02e, and 0.05e on going from CH₃Cl to CCl₄, which suggests that the decrease in the coordination energy with increasing the number of Cl atoms in the organohalide could be related to a decreased donor ability of the more halides rich molecules. The second step is the oxidative addition of the coordinated organohalide. In this case, the more Cl rich the organohalide the more favored is the oxidative addition step, see the ΔE_{OxAdd} in Table 4, with oxidative addition of

Table 4. Thermodynamics, in kcal·mol⁻¹, of the Oxidation of a [Mg]/TiCl₂ Species by Reaction with CH_nCl_{4-n} (n = 0–3)^a

	reaction	ΔE_{Coord}	ΔE_{OxAdd}	ΔE_{Tot}
1	[Mg]/TiCl ₂ + CH ₃ Cl → [Mg]/TiCl ₃ CH ₃	-15.9	-16.2	-32.1
2	[Mg]/TiCl ₂ + CH ₂ Cl ₂ → [Mg]/TiCl ₃ CH ₂ Cl	-15.6	-18.6	-34.2
3	[Mg]/TiCl ₂ + CHCl ₃ → [Mg]/TiCl ₃ CHCl ₂	-13.7	-20.9	-34.6
4	[Mg]/TiCl ₂ + CCl ₄ → [Mg]/TiCl ₂ CCl ₃	-11.8	-25.2	-37.0
5	[Mg]/TiCl ₂ + CH ₃ Cl → [Mg]/TiCl ₂ CH ₃ + Cl [•]			+2.2
6	[Mg]/TiCl ₂ + CH ₂ Cl ₂ → [Mg]/TiCl ₂ CH ₂ Cl + Cl [•]			-4.3
7	[Mg]/TiCl ₂ + CHCl ₃ → [Mg]/TiCl ₂ CHCl ₂ + Cl [•]			-11.4
8	[Mg]/TiCl ₂ + CCl ₄ → [Mg]/TiCl ₂ CCl ₃ + Cl [•]			-19.8

^a Entries 1–4 correspond to the organohalide oxidative addition associated with reactivation from Ti^{II} to Ti^{IV}, $\Delta E_{\text{Tot}} = \Delta E_{\text{Coord}} + \Delta E_{\text{OxAdd}}$. Entries 5–8 correspond to the organohalide radical dissociation, associated with reactivation from Ti^{II} to Ti^{III}.

CCl₄, with a ΔE_{OxAdd} of -25.2 kcal mol⁻¹, favored by 9.0 kcal mol⁻¹ over oxidative addition of CH₃Cl, with a ΔE_{OxAdd} of -16.2 kcal mol⁻¹. The trend in the ΔE_{OxAdd} correlates with the trend in the homolytic dissociation energy of the C–Cl bond in the organohalides considered, 80.6, 74.3, 67.1, and 58.6 kcal mol⁻¹ on going from CH₃Cl to CCl₄. In other words, the higher energy gain associated with the oxidative addition of CCl₄ relative to CH₃Cl can be related to the weaker C–Cl bond in CCl₄ relative to CH₃Cl. The final energy gain, $\Delta E_{\text{Tot}} = \Delta E_{\text{Coord}} + \Delta E_{\text{OxAdd}}$, reflects the trend of ΔE_{OxAdd} , although the differences between the various organohalides are reduced in magnitude.

Finally, since CCl₄ is also known for its radical chemistry, we evaluated the possibility that the Ti^{II} is oxidized to a Ti^{III} center by CCl₄ through homolytic dissociation of one C–Cl bond. For the sake of consistency we extended this calculation to all the organohalides considered, entries 5–8 in Table 4. The ΔE_{Tot} reported in Table 4, indicate that CH₃Cl and CH₂Cl₂, with a ΔE_{Tot} of +2.2 and -4.3 kcal mol⁻¹, are scarcely effective to oxidize the Ti^{II} center via a radical mechanism. CHCl₃ and, particularly, CCl₄, with a ΔE_{Tot} of -11.4 and -19.8 kcal mol⁻¹, are indeed quite capable of reoxidizing a Ti^{II} center via a radical mechanism. However, even considering an unfavorable entropic contribution for the oxidative addition mechanism, this reactivity seems to be clearly favored over the radical oxidation mechanism.

Concluding this section, our results suggest that with increasing the number of Cl atoms, the oxidation (reactivation) of a Ti^{II} center becomes thermodynamically more favored. This conclusion is in line with the well accepted concept that suitable promoters for ZN catalysts are usually multi chloro organohalides such as CHCl₃, CFCl₃, C₃H₂Cl₆, and C₃Cl₈,^{53,54} with a similar role of organohalides in the activation of V-based catalysts for ethylene polymerization,³⁴ and with several patents in the field of ZN-promoted ethene polymerization.^{38,55,56} Of course, after the Ti^{II} center has been reoxidized to Ti^{IV}, it can re-enter the catalytic cycle by activation steps such as those discussed in the previous sections.

Conclusions

In this study, we have investigated possible pathways for the activation/reduction of TiCl₄ adsorbed on a MgCl₂ cluster to Ti^{III} species, the possible deactivation/reduction of Ti^{III} species to Ti^{II} species, and finally the reoxidation of Ti^{II} species back to Ti^{IV} species. The main conclusions that emerge from our study are. First, the simple homolytic rupture of a dangling Ti–Cl bond of an adsorbed TiCl₄ molecule is of very high energy. The most effective reducing agent is AlEt₃ while AlCl₃ performs rather poorly. The species formed after rupture of a Ti–Cl bond is a [Mg]/Ti^{III}Cl₃[•] species with a coordinative vacancy. Second, direct transalkylation of [Mg]/TiCl₃[•] by AlEt₃ presents a rather low energy barrier, and leads to [Mg]/Ti^{III}Cl₂Et[•], which can be considered as the species from which chain growth can start via the classical monomer coordination/insertion mechanism of

Cossee.⁵⁷ Third, the [Mg]/Ti^{III}Cl₂Et[•] species, which can be considered as a model of the propagating species, is rather stable toward further reduction to Ti^{II} by either Cl or Et homolytic dissociation or abstraction by AlEt₃. In this context, the [Mg]/Ti^{III}Cl₂H[•] species that could be formed after a chain transfer reaction by either β -hydrogen elimination from the growing chain or by cleavage of the Ti–Et (polymeryl) bond by molecular hydrogen, is rather weaker and thus susceptible of reduction. Fourth, organohalides can easily coordinate to Ti^{II} species and then reoxidize them to Ti^{IV} species, thus reintroducing them into the catalytic cycle.

We underline that all these transformations always considered a single Ti–Et chloride species adsorbed on a MgCl₂ cluster reacting with standard other ingredients used industrially, thus providing a very simple and intuitive description of the possible changes in the oxidation states of Ti species active in ZN-catalysis. As a final remark, we are aware that these conclusions are based on reaction energies and do not consider energy barriers. This choice was dictated by the difficulty in modeling several reactions with a change in the spin state. However, considering that in many cases the reaction energies we calculated are very endothermic, this allows to rule them out even on a thermodynamics basis. In other cases, the reactions are thermodynamically highly favored, which can be taken as an indication supporting their feasibility.

Acknowledgment. We are grateful to one reviewer for very useful comments. NBL thanks Prof. H. Mirzadeh (Iran Polymer and Petrochemical Institute and Amirkabir University of Technology) for scientific support. LC thanks ENEA (www.enea.it) and the HPC team for support as for using the ENEA-GRID and the HPC facilities CRESCO (www.cresco.enea.it) Portici (Naples), Italy.

Supporting Information Available: Cartesian coordinates and energies in au of all the species discussed in the text, and the complete ref 41. This material is available free of charge via the Internet at <http://pubs.acs.org>.

References and Notes

- Ziegler, K. In *Nobel Lectures in Chemistry, 1963–1970*; Elsevier: Amsterdam, 1972; p 6.
- Natta, G. In *Nobel Lectures in Chemistry, 1963–1970*; Elsevier: Amsterdam, 1972; p 27.
- Albizzati, E.; Giannini, U.; Collina, G.; Noristi, L.; Resconi, L. In *Polypropylene Handbook*; Moore, E. P., Ed.; Hanser: Munich, Germany, 1996; p 11.
- Fregonese, D.; Glisenti, A.; Mortara, S.; Rizzi, G. A.; Tondello, E.; Bresadola, S. *J. Mol. Catal. A: Chem.* **2002**, *178*, 115.
- Stukalov, D. V.; Zakharov, V. A.; Potapov, A. G.; Bukatov, G. D. *J. Catal.* **2009**, *266*, 39.
- Stukalov, D. V.; Igor, L.; Zilberberg, V.; Zakharov, V. A. *Macromolecules* **2009**, *42*, 8165.
- Kim, S. H.; Somorjai, G. A. *J. Phys. Chem. B* **2000**, *104*, 5519.
- Zakharov, V. A.; Makhitarulin, S. I.; Poluboyarov, V. A.; Anufrienko, V. F. *Makromol. Chem.* **1984**, *185*, 1781.

- (9) Potapov, A. G.; Kriventsov, V. V.; Kochubey, D. I.; Bukatov, G. D.; Zakharov, V. A. *Macromol. Chem. Phys.* **1997**, *198*, 3477.
- (10) Martinsky, C.; Minot, C.; Ricart, J. M. *Surf. Sci.* **2001**, *490*, 237.
- (11) Taniike, T.; Terano, M. *Macromol. Rapid Commun.* **2007**, *28*, 1918.
- (12) Trubitsyn, D. A.; Zakharov, V. A.; Zakharov, I. I. *J. Mol. Catal. A: Chem.* **2007**, *270*, 164.
- (13) Credendino, R.; Busico, V.; Causà, M.; Barone, V.; Budzelaard, P. H. M.; Zicovich-Wilsons, C. *Phys. Chem. Chem. Phys.* **2009**, *11*, 6525.
- (14) Cavallo, L.; Guerra, G.; Corradini, P. *J. Am. Chem. Soc.* **1998**, *120*, 2428.
- (15) Denis, V.; Stukalov, Vladimir, A.; Zakharov; Zilberberg, I. L. *J. Phys. Chem. C* **2010**, *114*, 429.
- (16) Giannini, U.; Giunchi, G.; Albizzati, E.; Barbè, P. C. NATO ASI series. Series C, Mathematical and physical sciences, **1987**, *215*, 487.
- (17) Corradini, P.; Busico, V.; Guerra, G. *Monoalkene polymerization: stereospecificity, Comprehensive Polymer Science*; Pergamon Press: Oxford, U.K., 1989; Vol. 4.
- (18) Barino, L.; Scordamaglia, R. *Macromol. Theory Simul.* **1998**, *7*, 407.
- (19) Monaco, G.; Toto, M.; Guerra, G.; Corradini, P.; Cavallo, L. *Macromolecules* **2000**, *33*, 8953.
- (20) Boero, M.; Parrinello, M.; Terakura, K. *J. Am. Chem. Soc.* **1998**, *120*, 2746.
- (21) Seth, M.; Ziegler, T. *Macromolecules* **2003**, *36*, 6613.
- (22) Seth, M.; Margl, P. M.; Ziegler, T. *Macromolecules* **2002**, *35*, 7815.
- (23) Correa, A.; Piemontesi, F.; Morini, G.; Cavallo, L. *Macromolecules* **2007**, *40*, 9181.
- (24) Parodi, S.; Nocchi, R.; Giannini, U.; Barbè, P. C.; Scata, U. to Montedison S.p.A., 1982.
- (25) Barbè, C.; Cecchin, G.; Noristi, L. *Adv. Polym. Sci.* **1987**, *81*, 1.
- (26) Morini, G.; Balbontin, G.; Gulevich, Y. V.; Vitale, G. World Pat. Appl. to Basell Poliolefine Italia, 2002.
- (27) Busico, V.; Cipullo, R.; Polzone, C.; Talarico, G.; Chadwick, J. C. *Macromolecules* **2003**, *36*, 2616.
- (28) Busico, V.; Cipullo, R.; Monaco, G.; Talarico, G.; Vacatello, M.; Chadwick, J. C.; Segre, A. L.; Sudmeijer, O. *Macromolecules* **1999**, *32*, 4173.
- (29) Keii, T.; Suzuki, E.; Tamura, M.; Murata, M.; Doi, Y. *Makromol. Chem.* **1982**, *183*, 2285.
- (30) Soga, K.; Chen, S.-I.; Ohnishi, R. *Polym. Bull.* **1982**, *8*, 473.
- (31) Fuhrmann, H.; Herrmann, W. *Macromol. Chem. Phys.* **1994**, *195*, 3509.
- (32) Kashiwa, N.; Yoshitake, J. *Makromol. Chem.* **1984**, *185*, 1133.
- (33) Skalli, M. K.; Markovits, A.; Minot, C.; Belmajdoub, A. *Catal. Lett.* **2001**, *76*.
- (34) Adisson, E.; Deffieux, A.; Fontanille, M.; Bujadoux, K. *J. Polym. Sci., A: Polym. Chem.* **1994**, *32*, 1033.
- (35) Reinking, M. K.; Bauer, P. D.; Seyler, J. W. *Appl. Catal., A* **1999**, *189*, 23.
- (36) Winslow, L. N.; Klendworth, D. D.; Menon, R.; Lynch, M. W.; Fields, G. L.; Johnson, K. W. Patent WO/ 1996/031274 to Quantum Chemical Corporation, 1996.
- (37) Luo, H.-K.; Tang, R.-G.; Yang, H.; Zhao, Q.-F.; An, J.-Y. *Appl. Catal., A* **2000**, *203*, 269.
- (38) Farrer, D. K.; Dooley, K. A.; Moore, G. E.; Nobel, L. A. US Patent 09/912,171 to Eastman Chemical Company, 2003.
- (39) Stukalov, D. V.; Zakharov, V. A. *J. Phys. Chem. C* **2009**, *113*, 21376.
- (40) TURBOMOLE V6.2 2010, a development of University of Karlsruhe and Forschungszentrum Karlsruhe GmbH, 1989–2007, TURBOMOLE GmbH, since 2007; available from <http://www.turbomole.com>.
- (41) Frisch, M. J.; Trucks, G. W.; Schlegel, H. B. et al. Gaussian, Inc.: Pittsburgh PA, 2004.
- (42) Lee, C. Y., W.; Parr, R. G. *Phys. Rev. B* **1988**, *37*, 785.
- (43) Becke, A. D. *J. Chem. Phys.* **1993**, *98*, 1372.
- (44) Schäfer, A.; Huber, C.; Ahlrichs, R. *J. Chem. Phys.* **1994**, *100*, 5829.
- (45) Schäfer, A.; Horn, H.; Ahlrichs, R. *J. Chem. Phys.* **1992**, *97*, 2571.
- (46) Mole, T.; Jeffery, E. A. *Organoaluminum Compounds*; Elsevier Publishing Company: Amsterdam, 1972.
- (47) We used the experimental value since DFT is known to underestimate Al-alkyls dimerization energy severely (see ref 48). For instance, for AlEt₃ and AlCl₃ we calculated a dimerization energy of 5.2 and 22.1 kcal mol⁻¹, versus experimental values of 17 (see refs 46) and 30 (see ref 49) kcal mol⁻¹, respectively.
- (48) Willis, B. G.; Jensen, K. F. *J. Phys. Chem. A* **1998**, *102*, 2613.
- (49) Wade, K. *J. Chem. Educ.* **1972**, *49*, 502.
- (50) Tarazona, A.; Koglin, E.; Buda, F.; Coussens, B. B.; Renkema, J.; van Heel, S.; Meier, R. J. *J. Phys. Chem. B* **1997**, *101*, 4370.
- (51) Xie, T.; McAuley, K. B.; Hsu, J. C. C.; Bacon, D. W. *Ind. Eng. Chem. Res.* **1994**, *33*, 449.
- (52) Reed, A. E.; Curtiss, L. A.; Weinhold, F. *Chem. Rev.* **1988**, *88*, 899.
- (53) Beran, D. L.; Cann, K. J.; Jorgensen, R. J. Eur. Patent EP120501 to Union Carbide, 1984.
- (54) Nicoletti, J.W.; ; Cann, K.J.; ; Karol, F. J. Eur. Patent EP0286001B1 to Union Carbide Corporation, 1991.
- (55) Daire, E. US Patent 967,081 to BP Chemical Limited: United Kingdom, 1999.
- (56) Zoeckler, M. T. C.; Schramm, K. D. N.; Smale, M. W. C. Eur. Patent 99308944.0 to Union Carbide Corporation: 2000.
- (57) Cossee, P. *J. Catal.* **1964**, *3*, 80.